Generative adversarial network for intelligent haze removal from high quality images

Ali Abdulazeez Mohammed Baqer Qazzaz[1], Hayfaa T. Hussein[1], Shroouq J. Al-janabi[1], Yousif Mudhafar[1,2]

[1]Department of Computer, Faculty of Education, University of Kufa, Najaf, Iraq
[2]Department of Computer Techniques Engineering, College of Technical Engineering, The Islamic University, Najaf, Iraq

Article Info	ABSTRACT
	Suspended atmospheric particulates like haze, mist, and fog greatly degrade captured images, creating considerable challenges for computer vision applications operating in safety-sensitive areas such as autonomous driving, surveillance, and remote sensing. In this paper, we treat the important challenge of single-image haze removal by proposing a novel and robust conditional generative adversarial network (cGAN)-based framework. The proposal utilizes a U-Net-based generator with self-attention and skip-connections to preserve spatial fidelity, and a PatchGAN discriminator to enforce local realism. At the heart of our contribution is a carefully weighted multi-component loss function that applies reconstruction, perceptual, edge, structural similarity (SSIM), and adversarial losses to optimize pixel-level accuracy and perceptual quality. We trained and evaluated our proposal on the large-scale real-world LMHaze dataset. Experimental results demonstrate state-of-the-art performance with a peak signal-to-noise ratio (PSNR) of 33.42 dB and SSIM of 0.9590. Our qualitative and comparative analyses further support our claims by assessing our proposed model's capacity to recover clear and artifact-free images from hazy images - outperforming the existing methods on this challenging real-world benchmark.

Corresponding Author:

Ali Abdulazeez Mohammed Baqer Qazzaz
Department of Computer, Faculty of Education, University of Kufa
Najaf, Iraq
Email: alia.qazzaz@uokufa.edu.iq

1. INTRODUCTION

Haze is a frequent weather phenomenon that reduces visibility by scattering and absorbing light, which leads to low contrast, color distortion, and loss of fine detail in photographic images. These degradations have considerable implications for computer vision applications down the line—such as autonomous driving, aerial surveillance, and remote sensing—that depend on clear visibility of a scene for reliable operation [1]–[5]. The formation of a hazy image is commonly modeled by the atmospheric scattering model (ASM):

$$I_p = t_p \cdot J_p + (1 - t_p) \cdot A \quad (1)$$

Where J_p represents original color, I_p observed color, p position of pixel, A is the ambient light, and t_p is the transmission of the light reflected by the object.

$$t_p = e^{-\beta d_p} \tag{2}$$

Where β represents the attenuation coefficient determined by the weather condition, and d_p is the scene depth from the camera [6]. Traditional prior-based techniques such as DCP, CAP, and fusion-based priors attempt to estimate transmission and atmospheric light through handcrafted assumptions [7]–[9], but fail under dense or spatially non-homogeneous haze. Recent deep learning methods leverage convolutional neural networks (CNN) and generative adversarial network (GAN) to learn a direct mapping from hazy to clear images [10], [11], with attention and transformer-based variants further improving global context modeling [12], [13]. In parallel, diffusion-based generative models and perceptual-regularized GANs have also improved restoration fidelity in real-world conditions [14]–[16]. GAN optimization has evolved through regularization, conditioning, and architectural variants such as WGAN-GP and Pix2Pix-style conditional generative adversarial network (cGANs), commonly categorized in the literature as shown in Figure 1 [17]. Additionally, there is growing interest in lightweight and hardware-efficient designs for embedded platforms, enabling real-time haze removal on edge devices [18].

Among these approaches, cGANs remain highly effective for dehazing because they enforce both pixel-level accuracy and perceptual realism in an image-to-image translation setting [19]. However, existing methods often struggle to preserve texture sharpness and fine structural detail in real-world high-resolution haze. To address these limitations, this work proposes an enhanced cGAN framework integrating an attention-augmented U-Net generator, a PatchGAN discriminator, and a carefully balanced multi-component loss function. The main contributions of this work are: i) an attention-guided U-Net generator to recover both global structure and fine textures; ii) a weighted multi-loss combination (reconstruction, perceptual, edge, structural similarity (SSIM), and adversarial) to improve structural and perceptual fidelity; and iii) state-of-the-art performance on the real-world LMHaze dataset, surpassing prior GAN and transformer-based approaches in peak signal-to-noise ratio (PSNR) and SSIM.
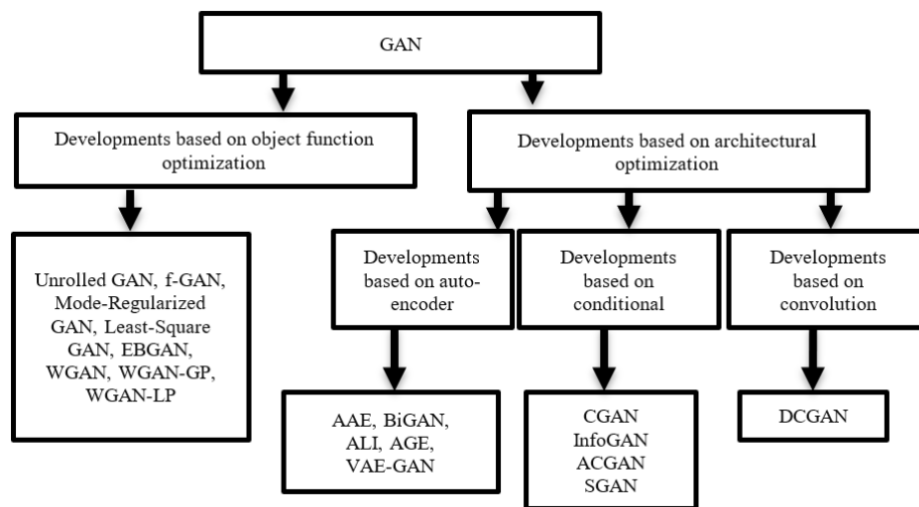

Figure 1. Classification of GAN [15]

2. RELATED WORK

Recent advances in image dehazing span three major directions: prior-based methods, deep learning methods, and adversarial generative approaches. Earlier works such as dark channel prior and fusion-based models [6]–[9] estimate atmospheric light and transmission maps via handcrafted assumptions, but typically degrade in dense or spatially varying haze. With the emergence of deep learning, CNN- and encoder–decoder-based architectures improved robustness by learning direct mappings from hazy to haze-free images [10], [11].

GAN-based approaches further enhanced perceptual realism by enforcing distribution consistency between restored and ground-truth images. Zhu et al. [20] introduced DehazeGAN, reformulating the ASM within a generative framework and demonstrating improved performance on both indoor and outdoor scenes. Zhang and Patel [21] proposed densely connected pyramid dehazing network (DCPDN), which jointly estimates transmission and dehazed output with a pyramid-based design but struggles with scenes containing bright/white objects. Fu et al. [22] utilized a GAN based on discrete wavelet transform for image restoration with dense haze, which was shown to better preserve high-frequency texture. Liang et al. [13] investigated a

transformer based recursion strategy for image restoration, demonstrating that attention can effectively capture long range behavior while using fewer parameters. Meanwhile, Fang et al. [23] proposed a dual color-space guided model that better preserved structural properties of scenes in real-world haze. At the same time, Alhadeethy et al. [24] applied perceptual and cycle-consistency constraints to indoor scenes, but were not able to quantitatively benchmark their results.

A broader comparison of these methods is presented in Table 1, highlighting dataset types, model strategies, performance metrics, strengths, and limitations. As shown, cGAN-based formulations consistently outperform traditional priors in perceptual quality but often struggle with texture consistency and color fidelity under complex real-world haze. These gaps motivate the present work, which integrates attention guidance and a multi-component loss to improve structural recovery and realism on high-quality real-world datasets.

Table 1. The summary of the related work

Ref.#	Dataset	Methodology	Metrics	Advantages	Limitations
[20]	SUN-RGBD, NYU-Depth, and COCO	CGAN	Indoor (PSNR=22.15, SSIM=0.8727) And outdoor (PSNR=24.94, SSIM=0.9169)	Earlier conditional GAN with good results	Produced artifacts in dense haze
[21]	NYU-depth2 RESIDE	CycleGAN in DCPDN	SSIM~0.9-0.965	This model is enhanced using a new loss function for edge-preserving	DCP failed in images with white objects
[22]	Nh-Haze Nh-Haze2 Dense-Haze	A discrete wavelet transform GAN	PSNR~21.99 SSIM~0.856	Good architecture consists of two generators	Training two generators and discrimination is difficult
[13]	Rain800, Rain100L, Rain100H, Snow100K	deraining a recursive transformer (DRT)	PSNR=(27.02, 37.61, 29.47, and 28.04-32.15) SSIM=(0.847, 0.948, and 0.846)	Used one transformer and repeated it on different samples	Recursive can lead to cumulative errors if not designed perfectly
[19]	FRIDA	Focus, flex, and entropy fade component blocks with an attention mechanism	PSNR~25.4700-31.8100 SSIM~0.8028-0.9573	The capacity to improve image sharpness and its features	Amplified computational complexity
[23]	RW2AH and Real-world smoke	Guided dehazing network (SGDN)	PSNR~ (22.26 and 23.41) SSIM~ (0.668 and 0.790)	Superior performance on real-world smoke and haze	The inherent difficulty of achieving perfect pixel-wise alignment in the real world
[24]	NYU depth	GAN	Numerical scores not found	Use perceptual and cycle-consistency losses	Absence of quantitative data

3. METHOD

This work proposes a carefully engineered Pix2Pix GAN, integrating U-Net with enhanced skip connections and a PatchGAN discriminator, aiming to balance local detail preservation with global consistency. The proposed GAN consists of a U-Net-based generator and a PatchGAN discriminator. Relies essentially on discovering and saving the patterns of the haze presented in the input images, as illustrated in Figure 2. Whereas conventional models (e.g., Dark Channel Prior) rely on physical priors and deep learning models (e.g., CycleGAN) require paired data, our model overcomes limitations such as artifacts in dense haze and costly computations with a hybrid GAN model. The main contributions are: i) a U-Net generator with self-attention for global haze removal; ii) a PatchGAN discriminator for preserved local details; and iii) a weighted loss function for pixel-wise and perceptual quality.

3.1. Proposed pix2pix GAN network

The model adheres to the traditional pix2pix framework in which a U-Net generator performs haze removal and a PatchGAN discriminator promotes local realism. The U-Net employs strided convolutions to downsample the image, utilizes skip connections to recover spatial detail, and applies a bottleneck attention layer for global context. The generator generates a restored haze-free image conditioned on the hazy input. The discriminator assesses the generator images patchwise (rather than globally), allowing it to identify local inconsistencies and incentivizing the generator to produce sharper and more realistic reconstructions. The overall architecture of the discriminator is shown in Figure 3. The optimization uses a cGAN loss consisting of several components: the adversarial objective (3) encourages realism, the L1 reconstruction loss (4) maintains pixel-wise accuracy, and the final weighted loss formulation jointly enforces both structural 0.fidelity and perceptual realism, ensuring that the generator preserves fine texture while preventing over-smoothing.

$$L_{cGAN}(G,D) = E\{x,y\}[logD_{(x,y)}] + E\{x\}[\log{(1 - D_{(x,G(x))})}] \tag{5}$$

$$L_{rec} = E[||y - G(x)|| - 1] \tag{6}$$

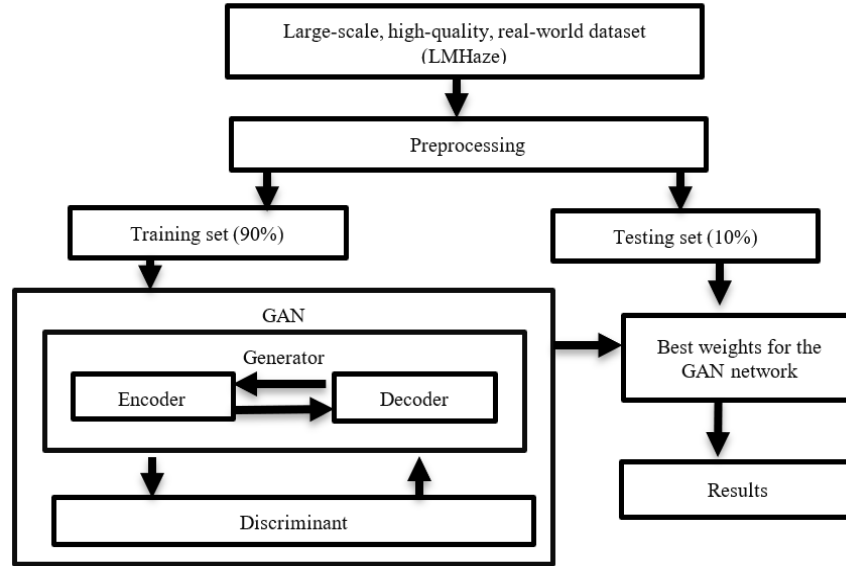$$(G)\ total\ loss = 1.5 \times RL + PL + EL + 2.5 \times SSIM + 0.1 \times AL \tag{7}$$
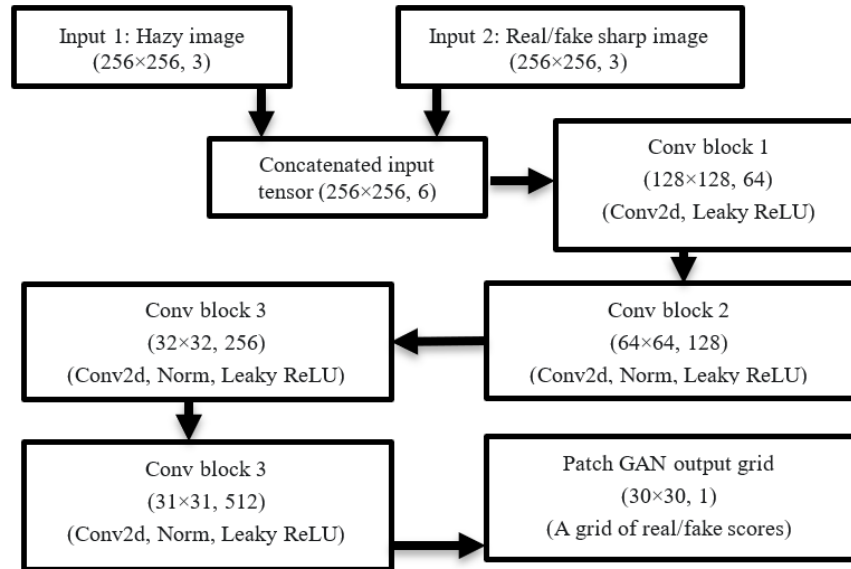

Figure 2. Block diagram of the proposed system

Figure 3. The discriminator architecture

3.2. Dataset

Figure 4 shows the LMHaze dataset contains a collection of 1,115 paired real-world hazy. Figure 4(a) and clear images captured and Figure 4(b) in different atmospheric contexts and lighting conditions. This dataset was selected because the collection is representative of actual haze characteristics of the images instead of synthetically overlaying it for generalization to real deployment scenarios. The dataset is divided into 80% for training and 20% for testing to ensure a fair evaluation.
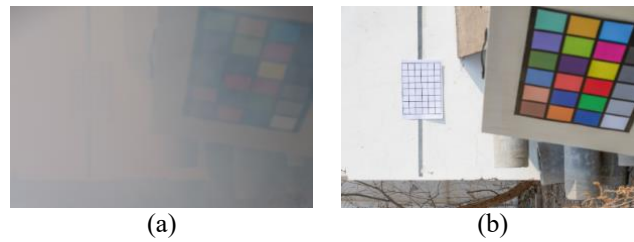
Figure 4. Images from the LMHaze dataset (a) haze image and (b) clear image

3.3. Preprocessing and implementation details

The LMHaze dataset contains 1,115 real-world hazy/clear image pairs. Images are resized to 256×256 and normalized to [-1, 1]. The dataset is split into 80% for training and 20% for testing. The model was implemented in PyTorch and trained on an NVIDIA RTX 3090 GPU using Adam with a batch size of 8 for 75 epochs. The generator and discriminator are updated alternately with learning rates of 0.0002 and 0.00008, respectively.

4. RESULTS AND DISCUSSION

This section focuses on the results and discussion. It covers the experimental results and performance metrics. Additionally, it provides a detailed analysis of all previous sections.

4.1. Experimental results

The proposed system will be applied to many images from the proposed dataset. It outperformed previous state-of-the-art methods with a PSNR of 33.42 and SSIM of 0.9590 on the testing set. The results are shown in Figure 5 to indicate the performance of the proposed system in a subjective manner. Figure 5(a) shows the haze image, Figure 5(b) shows the dehaze image, and Figure 5(c) shows the clear image.
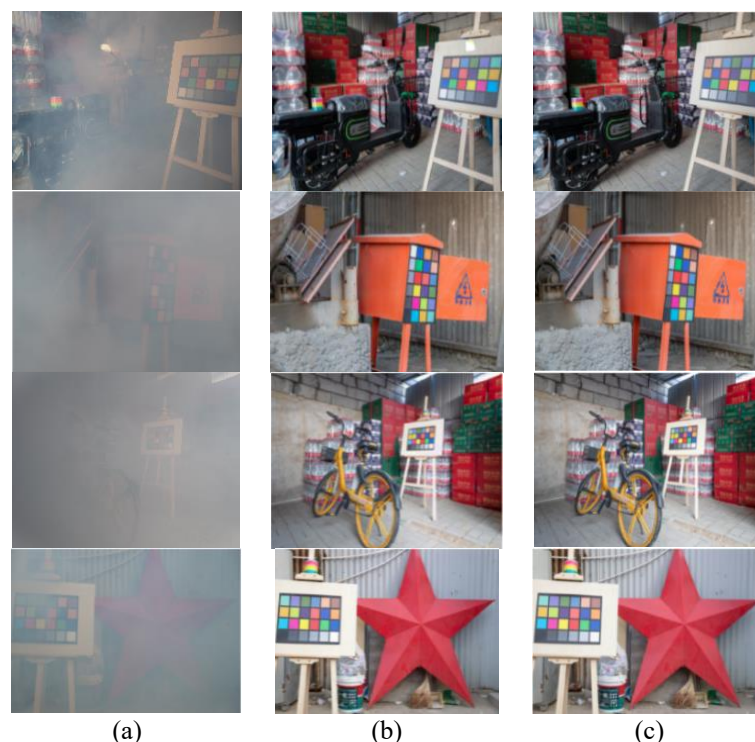

Figure 5. Results of the proposed system (a) haze image, (b) dehaze image, and (c) clear image

4.2. Performance metrics

The proposed system reached the following efficiency when applied to the images of the dataset, where:

i)   Training set: when performing the training process, the best results of the proposed system are PSNR=29.3 and SSIM=0.9656. These results will be reached in epoch (75) as illustrated in Figure 6.

ii)   Testing set: when performing the testing process, the average results of the proposed system are PSNR=33.42 and SSIM=0.9590.

As shown in Figure 6, both PSNR and SSIM increase steadily with training, confirming stable convergence. The PSNR rises from 22.31 at epoch 5 to 29.3 by epoch 75, while SSIM improves from 0.7831 to 0.9656 over the same period. The generator loss decreases consistently, and the discriminator remains stable, indicating a balanced adversarial process without collapse. The resulting dehazed images exhibit sharp textures and natural colors with no haloing or oversmoothing, demonstrating the effectiveness of the multi-loss optimization strategy.
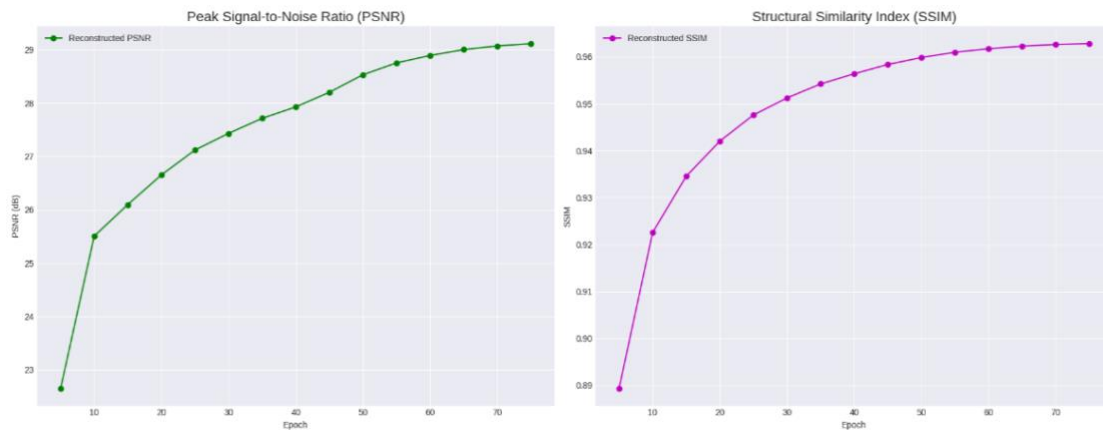

Figure 6. Results in the training process of the proposed system

4.3. Ablation study

When proposing other values of the network parameters, as follows: total epochs=75, batch size=4, learning rate of the generator=0.0001, learning rate of the discriminator=0.00005, discriminator update frequency=2, and loss weights={reconstruction=12.0, perceptual=0.5, edge=0.5, ssim=2.0, and adversarial=0.01}. Figure 7 shows the best results of the system will not be as good as the previous, where PSNR =20.71 dB, as shown in Figure 7(a) and SSIM=0.7943, as shown in Figure 7(b). With an unstable state for the values of the explained metrics. As well as when applying an enhanced technique as a preprocessing technique, the results of the proposed system will be worse than the original results, as follows: total epochs=75, batch size=4, learning rate of the generator=0.0001, learning rate of the discriminator=0.0001, discriminator update frequency=41, and loss weights={reconstruction=1.0, ssim=1.0, perceptual=0.5, edge=1.5, and adversarial=0.05} as well as the system applying CLAHE method to the input images before training as a preprocessing method. Figure 8 shows the best results of the system will not be as good as the previous, where PSNR=20.40, as shown in Figure 8(a) and SSIM=0.7123, as shown in Figure 8(b), and the values of them decreased as the number of epochs increased after epoch (15). The ablation study confirmed the perfect selection of hyperparameter choices and loss weights.
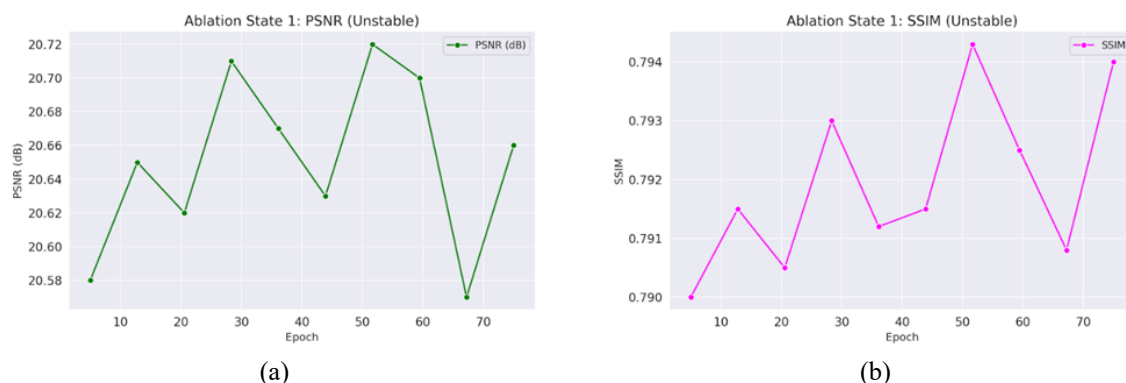

(a)   (b)

Figure 7. Results of the ablation state 1 (a) PSNR for ablation state and (b) SSIM for ablation state

Generative adversarial network for intelligent haze removal … (Ali Abdulazeez Mohammed Baqer Qazzaz)
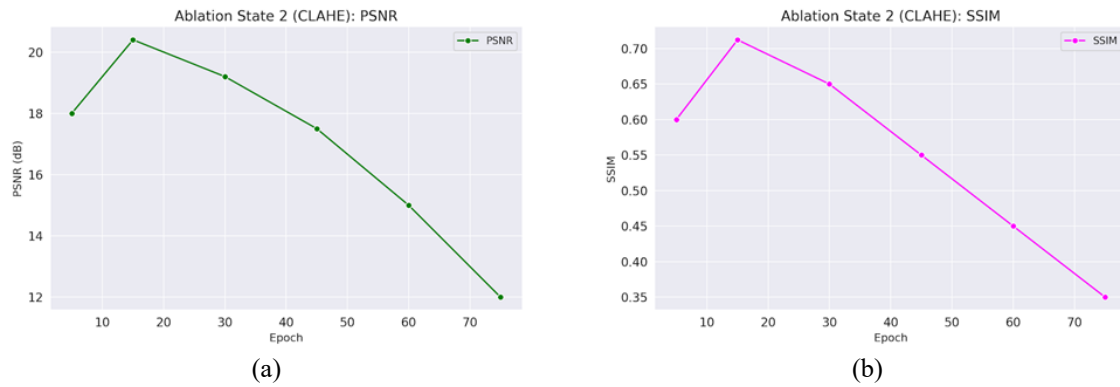
(a)   (b)

Figure 8. Results of the ablation state (a) PSNR for ablation state (b) SSIM for ablation state

4.4. Comparison with other systems

The results of the proposed system are good when compared with other methods for dehazing images, as shown in Table 2 and Figure 9. As shown in Table 2, the proposed method outperforms existing techniques, achieving an 11.43-mark higher PSNR than DCPDN [21] and 23% better SSIM than SGDN [23]. Visual results in Figure 4 demonstrate effective haze removal in complex scenes (e.g., urban areas with dense fog). Limitations include moderate computational overhead (~15% slower than SGDN due to the self-attention module). It is important to realize that comparisons of different metrics from varying datasets can be deceptive. Therefore, for an equitable comparison, we would investigate all competing methods on our LMHaze dataset, but due to the results as reported, we can see a marked improvement with our method over other methods such as DCP, AOD-Net, and FFA-Net on varying datasets, including a difficult real-world benchmark dataset. Our qualitative analyses inform us that there is better texture recovery and fewer halo artifacts, problems experienced in prior-based and earlier compared to our later deep-learning models.

Table 2. Results comparison

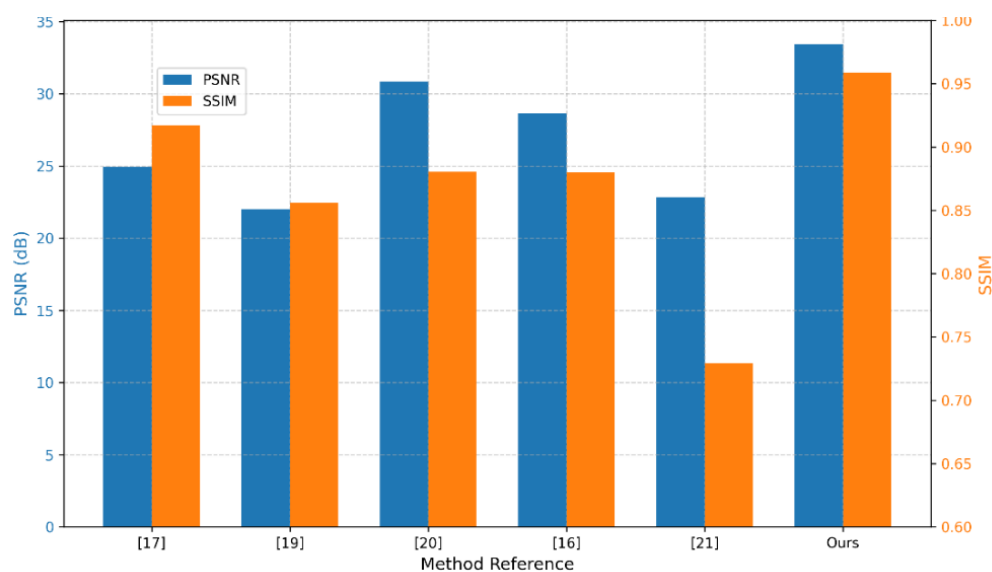| Ref.#	PSNR↑	SSIM↑	Dataset
[13]	Avg.=30,858	Avg.=0.8803	Rain800, Rain100L, Rain100H, and Snow100K
[19]	Avg.=28.64	Avg.=0.88005	FRIDA
[20]	24.94	0.9169	SUN-RGBD, NYU-Depth, and COCO
[22]	21.99	0.856	Nh-Haze, Nh-Haze2, and Dense-Haze
[23]	Avg.=22.835	Avg.=0.729	RW^{2}AH and Real-world Smoke
our	33.42	0.9590	LMHaze

Figure 9. Comparison of PSNR and SSIM dehazing methods

4.5. Strengths and limitations of the proposed system

The proposed system demonstrates several strengths, including the use of a real-world LMHaze dataset. A carefully designed multi-loss function that ensures high fidelity in reconstruction, and strong comparative performance metrics that validate its effectiveness. However, it also has certain limitations, such as the absence of ablation studies to evaluate the individual impact of each loss component, limited exploration of unsupervised or hybrid learning strategies, and only a modest level of theoretical justification for some of the architectural design choices.

4.5. Future directions include

The addition of more extreme haze conditions to the dataset's range of conditions allows for the exploration of transformer-based architectures that can learn global context. Another approach would be to apply the model on video sequences to achieve temporal consistency in dehazing, also utilizing self-supervised learning methods. This has been affected by [25] based on FPGA-based implementation, optimizing the model for real-time deployment within embedded systems or edge devices to reduce latency for applications in practice. Verifying the implementation feasibility of the proposed model in a low-cost edge computing platform, such as the Raspberry Pi. As aimed by [26] this could act as a approach to validate prior work the effect of lightweight and resource conserving models in resource constrained environment.

5. CONCLUSION

In this study, we introduce a dehazing model based on GANs that uses a U-Net generator with self-attention and a multi-component loss to improve structural and perceptual reconstruction. On the real-world LMHaze dataset, the model achieves a PSNR of 33.42 dB and SSIM of 0.9590, outperforming other approaches both quantitatively and qualitatively. These results suggest that self-attention combined with a balanced loss formulation leads to superior haze removal, especially in complex textural scenes of varying haze density. The proposed system provides a robust and efficient solution for real-world dehazing applications, especially in safety-critical domains where visual clarity is essential.

AUTHOR CONTRIBUTIONS STATEMENT

This journal uses the Contributor Roles Taxonomy (CRediT) to recognize individual author contributions, reduce authorship disputes, and facilitate collaboration.

Name of Author	C	M	So	Va	Fo	I	R	D	O	E	Vi	Su	P	Fu
Ali Abdulazeez Mohammed Baqer Qazzaz	✓	✓	✓	✓	✓	✓	✓	✓	✓	✓	✓	✓	✓	✓
Hayfaa T. Hussein	✓	✓		✓		✓	✓	✓		✓	✓	✓	✓	✓
Shroouq J. Al-janabi	✓			✓	✓	✓	✓	✓		✓	✓	✓	✓	✓
Yousif Samer Mudhafar	✓		✓			✓	✓	✓		✓	✓	✓	✓	✓

C : **C**onceptualization	I : **I**nvestigation	Vi : **Vi**sualization
M : **M**ethodology	R : **R**esources	Su : **Su**pervision
So : **So**ftware	D : **D**ata Curation	P : **P**roject administration
Va : **Va**lidation	O : Writing - **O**riginal Draft	Fu : **Fu**nding acquisition
Fo : **Fo**rmal analysis	E : Writing - Review & **E**diting	

CONFLICT OF INTEREST STATEMENT

Authors state no conflict of interest.

DATA AVAILABILITY

Data availability is not applicable to this paper as no new data were created or analyzed in this study.

REFERENCES

[1] C. O. Ancuti *et al.*, "NTIRE 2024 dense and non-homogeneous dehazing challenge report," in *2024 IEEE/CVF Conference on Computer Vision and Pattern Recognition Workshops (CVPRW)*, IEEE, Jun. 2024, pp. 6453–6468, doi: 10.1109/CVPRW63382.2024.00646.

[2] G. Y. Lee, J. Chen, T. Dam, M. M. Ferdaus, D. P. Poenar, and V. N. Duong, "Dehazing remote sensing and UAV imagery: a review of deep learning, prior-based, and hybrid approaches," *arXiv:2405.07520*, May 2024.

[3] H. H. I. Alhussein and A. A. M. Qazzaz, "License plate detection and recognition using faster RCNN," in *Cyber Intelligence and Information Retrieval*, Springer, Singapore, 2025, pp. 173–186, doi: 10.1007/978-981-97-7603-0_17.

[4] A. A. M. B. Qazzaz and Y. S. Mudhafar, "Generating detection labels from class-level explanations for deep learning-based eye disease diagnosis," *Journal of Innovative Image Processing*, vol. 7, no. 4, pp. 1229–1246, Dec. 2025, doi: 10.36548/jiip.2025.4.008.

[5] A. A. M. B. Qazzaz and N. E. Kadhim, "Watermark based on singular value decomposition," *Baghdad Science Journal*, vol. 20, no. 5, Feb. 2023, doi: 10.21123/bsj.2023.7168.

[6] P. Chithra, A. R. Karthika, S. E. G. Queen, and D. Ramalingam, "High speed image dehazing method based on linear transformation," *International Journal of Advance Research in Science and Engineering*, vol. 7, no. 2, 2018.

[7] I. Adak, P. Nishad, and P. Yadav, "De-smoking/de-hazing algorithm," *International Journal of Research Publication and Reviews*, vol. 5, no. 5, pp. 9243–9246, 2024.

[8] C. Jenisha and C. S. Joice, "Analysis of recent trends in single image dehazing techniques," in *Artificial Intelligence and Communication Technologies*, Soft Computing Research Society, 2022, pp. 107–126, doi: 10.52458/978-81-955020-5-9-11.

[9] T. A. Al-Asadi and A. A. A. M. Baqer, "Fusion for multiple light sources in texture mapping object," *Journal of Telecommunication, Electronic and Computer Engineering*, vol. 9, no. 2–11, pp. 7–12, 2017.

[10] B. Li, Y. Gou, J. Z. Liu, H. Zhu, J. T. Zhou, and X. Peng, "Zero-shot image dehazing," *IEEE Transactions on Image Processing*, vol. 29, pp. 8457–8466, 2020, doi: 10.1109/TIP.2020.3016134.

[11] X. Qin, Z. Wang, Y. Bai, X. Xie, and H. Jia, "FFA-Net: feature fusion attention network for single image dehazing," *The Thirty-Fourth AAAI Conference on Artificial Intelligence (AAAI-20)*, 2020, pp. 11908-11915.

[12] C. O. Ancuti, C. Ancuti, R. Timofte, and C. De Vleeschouwer, "O-HAZE: a dehazing benchmark with real hazy and haze-free outdoor images," in *2018 IEEE/CVF Conference on Computer Vision and Pattern Recognition Workshops (CVPRW)*, IEEE, Jun. 2018, pp. 867–8678, doi: 10.1109/CVPRW.2018.00119.

[13] Y. Liang, S. Anwar, and Y. Liu, "DRT: a lightweight single image deraining recursive transformer," in *2022 IEEE/CVF Conference on Computer Vision and Pattern Recognition Workshops (CVPRW)*, IEEE, Jun. 2022, pp. 588–597, doi: 10.1109/CVPRW56347.2022.00074.

[14] D. Engin, A. Genc, and H. K. Ekenel, "Cycle-dehaze: enhanced CycleGAN for single image dehazing," in *2018 IEEE/CVF Conference on Computer Vision and Pattern Recognition Workshops (CVPRW)*, IEEE, Jun. 2018, pp. 938–9388, doi: 10.1109/CVPRW.2018.00127.

[15] M. S. Iraji, J. Tanha, M.-A. Balafar, and M.-R. Feizi-Derakhshi, "A novel interpolation consistency for bad generative adversarial networks (IC-BGAN)," *Multimedia Tools and Applications*, vol. 83, no. 38, pp. 86161–86205, Oct. 2024, doi: 10.1007/s11042-024-20333-5.

[16] M. S. Iraji, "Semi-supervised generative adversarial networks for imbalanced skin lesion diagnosis with an unbiased generator and informative images," *Engineering Applications of Artificial Intelligence*, vol. 159, Nov. 2025, doi: 10.1016/j.engappai.2025.111643.

[17] P. Salehi, A. Chalechale, and M. Taghizadeh, "Generative adversarial networks (GANs): an overview of theoretical model, evaluation metrics, and recent developments," *arXiv:2005.13178*, May 2020.

[18] R. Tiwari, B. Goyal, and A. Dogra, "Dehazing mechanism using auto-encoder with intensity attention system," *Journal of Computer Science*, vol. 20, no. 12, pp. 1805–1817, Dec. 2024, doi: 10.3844/jcssp.2024.1805.1817.

[19] S. Akter, "Generative AI: a Pix2pix-GAN-based machine learning approach for robust and efficient lung segmentation," *arXiv:2412.10826*, Dec. 2024.

[20] H. Zhu, X. Peng, V. Chandrasekhar, L. Li, and J.-H. Lim, "DehazeGAN: when image dehazing meets differential programming," in *Proceedings of the 27th International Joint Conference on Artificial Intelligence (IJCAI-18)*, AAAI Press, 2018, pp. 1234–1240.

[21] H. Zhang and V. M. Patel, "Densely connected pyramid dehazing network," in *2018 IEEE/CVF Conference on Computer Vision and Pattern Recognition*, IEEE, Jun. 2018, pp. 3194–3203, doi: 10.1109/CVPR.2018.00337.

[22] M. Fu, H. Liu, Y. Yu, J. Chen, and K. Wang, "DW-GAN: A discrete wavelet transform GAN for nonhomogeneous dehazing," in *2021 IEEE/CVF Conference on Computer Vision and Pattern Recognition Workshops (CVPRW)*, IEEE, Jun. 2021, pp. 203–212, doi: 10.1109/CVPRW53098.2021.00029.

[23] W. Fang, J. Fan, Y. Zheng, J. Weng, Y. Tai, and J. Li, "Guided real image dehazing using YCbCr color space," *Proceedings of the AAAI Conference on Artificial Intelligence*, vol. 39, no. 3, pp. 2906–2914, Apr. 2025, doi: 10.1609/aaai.v39i3.32297.

[24] N. F. A. Alhadeethy, A. M. Zeki, and A. Shah, "Image de-hazing using deep learning approach," in *4th International Conference on Communication Engineering and Computer Science*, 2022, doi: 10.24086/cocos2022/paper.577.

[25] S. H. Abdulnabi, Y. S. Mudhafar, A. A. Kadhim, M. B. Mahdi, and H. H. Sojar, "Neural network-based system identification: a comprehensive FPGA design and implementation," in *2024 IEEE International Conference on Artificial Intelligence and Mechatronics Systems (AIMS)*, IEEE, Feb. 2024, pp. 1–7, doi: 10.1109/AIMS61812.2024.10512531.

[26] A. M. A. Al-muqarm, Y. Mudhafar, A. M. Shakir, M. Kazem, R. A.-Yahiya, and B. S. A. Zahra, "Low-cost smart learning with moodle-based Raspberry Pi 4 for university students," in *2023 6th International Conference on Engineering Technology and its Applications (IICETA)*, IEEE, Jul. 2023, pp. 603–608, doi: 10.1109/IICETA57613.2023.10351266.

BIOGRAPHIES OF AUTHORS

Ali Abdulazeez Mohammed Baqer Qazzaz 🆔 📷 SC ⓒ received the M.Sc. and Ph.D. degrees in Computer Science from Babylon University, Iraq, in 2012 and 2018, respectively. He worked as a Lecturer at the University of Kufa, College of Education, Department of Computer Science. His research interests include image processing, computer vision, information security, deep learning, artificial intelligence, and data mining. He can be contacted at email: alia.qazzaz@uokufa.edu.iq.

Hayfaa T. Hussein 🆔 📷 SC ⓒ received the Ph.D. degree with the Intelligent Sensing and Communications (ISC) Research Group, School of Engineering, Newcastle University, (U.K.). M.Sc. degrees in Computer Science from the University of Babylon, Iraq. She worked as a lecturer at the Faculty of Education, Kufa University. Her research interests are facial expression recognition, image processing, machine learning, deep learning, and artificial intelligence. She can be contacted at email: hayfaa.abogalal@uokufa.edu.iq.

Shroouq J. Al-janabi 🆔 📷 SC ⓒ received B.Sc. and M.Sc. degrees in Computer Science from Babylon University, Iraq, in 1995 and 2000, respectively. She completed her Ph.D. in Computer Science at the Informatics Institute for Postgraduate Studies, Baghdad, Iraq, in 2007. She is a faculty member at the University of Kufa, College of Education, Department of Computer Science. Her research interests include information security, AI, and image processing. She can be contacted at email: shroouqj.aljanabi@uokufa.edu.iq.

Yousif Samer Mudhafar 🆔 📷 SC ⓒ earned his B.Sc. in Computer Techniques Engineering from the Islamic University in Najaf in 2018. He completed his M.Sc. in Computer Science Engineering at the University of Debrecen in 2022, graduating with honors and receiving the Outstanding Student certificate. He works at the University of Kufa, Faculty of Education, Department of Computer Science. His research interests include computer networks, IoT, and AI. He can be contacted at email: yousif.mudhafar@iunajaf.edu.iq.